VOL. 25, NO. 1, 2026, 27-34
elektrika.utm.my
ISSN 0128-4428

ELEKTRIKA
Journal of Electrical Engineering

Comparative Metaheuristic Optimization for Sizing Grid-Connected Hybrid Renewable Systems: A Libya Case Study

Munir Ganbasha[1,2], **Razman Ayop**[1*], **Mohd Junaidi Abdul Aziz**[1], **Mohd Rodhi Bin Sahid**[1], **Mohammad Al Takrouri**[1] and **Firdaus Ishak**[1]

[1]Faculty of Electrical Engineering, Universiti Teknologi Malaysia, 81310 UTM Skudai, Johor, Malaysia.
[2]Department of Electrical Engineering, Faculty of Engineering, Elmergib University, Al- Khums, Libya.

[*]Corresponding author: razman.ayop@utm.my

Abstract: Hybrid renewable energy system (HRE) sizing is vital for maximizing both economic and environmental performance in grid-connected systems. This study develops a comparative optimization framework for an HRE serving a camp in the southeastern region of Libya, integrating photovoltaic (PV) arrays, wind turbines (WT), battery storage systems (BT), fuel cells (FC), hydrogen tanks (HT) and an Electrolyzer (EL). Three objective functions, Levelized Cost of Energy (LCOE), Grid Reliance Fraction (GRF) and Pollutant Emission Coefficient (PEC), are employed to quantify techno-economic efficiency and environmental impact. To this end, three widely used metaheuristic algorithms; Particle Swarm Optimization (PSO), Genetic Algorithm (GA) and Grey Wolf Optimizer (GWO), are employed under identical settings to identify optimal system configurations. Each algorithm is run for a fixed number of iterations, and their diversity and convergence behaviors are monitored to ensure a fair benchmark. The comparative results show that PSO yields the most cost-effective design, achieving an LCOE of $0.1448/kWh, a reduction of 13.5% and 1.3% relative to GA and GWO, respectively and a GRF of 15.73%. These findings demonstrate that PSO strikes the best balance between cost, reliability and computational efficiency for this HRE case study. The framework and insights presented here can guide planners and engineers in selecting the most suitable optimization method for sustainable energy-system design.

Keywords: Hybrid renewable energy, Hydrogen storage system, Energy management system, Metaheuristic algorithm

Article History: received 29 May 2025; accepted 12 February 2026; published 30 April 2026
Digital Object Identifier 10.11113/elektrika.v25n1.752

1. INTRODUCTION

The growth in global energy demand reflects rising populations, economic development and industrial activity. Yet continued reliance on coal, oil and natural gas has driven environmental degradation and resource depletion [1]. In Libya, an aging transmission network struggles to supply dispersed desert communities, resulting in high losses, frequent outages and rural electrification gaps. At the same time, the country benefits from some of the highest solar irradiance rates worldwide (6-8 kWh/m²/day) and notable coastal wind resources [2]. Deploying utility-scale RE plants would alleviate these challenges, reduce fossil-fuel dependence and support Libya's transition to a more sustainable energy system [3].

Global advancements in renewable energy technology have facilitated the establishment of localized, self-sufficient microgrid networks. Microgrids typically integrate several generation sources, such as photovoltaic (PV) systems and wind turbines (WT), with energy-storage systems (ESS) to enhance reliability and sustainability. Battery (BT) storage systems are well established, while hydrogen storage systems (HSS) offer large-scale capacity by converting surplus RE into compressed hydrogen and reconverting it via fuel cells (FC) during shortages [4]. By integrating diverse renewables and a hybrid hydrogen-battery ESS, microgrids can mitigate intermittency, regional variability and high upfront costs. However, designing efficient, cost-effective hybrid renewable energy (HRE) requires optimally sizing its nonlinear mix of generation, storage and control components under multiple objectives. Consequently, a range of classical and metaheuristic optimization techniques has been developed to address these complex design challenges [5]. Many studies have investigated the management and sizing of HRE systems that combine HSS and BT storage system, using diverse methods to identify optimal strategies.

V. Dargahi et al. [6] propose PSO-based method for optimal sizing and operation of an islanded hybrid microgrid integrating PV arrays, WT, pumped hydro storage and FC. Their strategy employs hourly wind, solar, and load data to minimize total operational cost, fuel consumption and CO_2 emissions, while enhancing system reliability through effective coordination of renewable generation and storage. Yan et al. [7] propose a modified bio-inspired optimization algorithm, an enhanced PSO, to size and operate an off-grid WT/PV/HSS microgrid. They

optimize designs using total annual cost (TAC), COE and LPSP. The results confirm the new algorithm's superiority over standard PSO and identify system configuration achieving the lowest TAC and COE at 2% unavailability. Agoundedemba et al. [8] propose a hybrid optimization framework that combines a genetic algorithm (GA) for optimal sizing with model predictive control for real-time energy management system (EMS) of a PV/WT/Fc/BT microgrid. This system aims to minimize the cost of energy (COE), the Net present cost (NPC) and loss of power supply probability (LPSP), while maintaining the BT state-of-charge (SOC) within safe limits.

Modu et al. [9] presents an improved Salp Swarm Algorithm (LSC-SSA) to determine the optimal sizing and EMS for a grid-connected hybrid microgrid. This microgrid integrates PV panels, WTs, EL, FC with compressed hydrogen storage and a BT storage system. Abeg et al. [10] propose a new meta-heuristic algorithm, MEXA, inspired by GA and grey wolf optimizer (GWO) to optimize both the sizing and operation of an off-grid hybrid microgrid serving economic zones in Bangladesh. This microgrid comprises PV, WT, BT storage, a diesel generator and EL. The authors also develop EMS to coordinate these components. The study aims to minimize installation and operating costs, maximize RE utilization, ensure reliable supply and convert surplus power into hydrogen. Yazdani et al. [11] apply a multi-objective optimization framework, minimizing NPC, LPSP, and CO_2 emissions, to determine the optimal sizes of grid connection PV, WT, micro-gas turbines, HSS and BT for a large off-grid/on-grid energy complex. They simulate configurations in HOMER, extract the Pareto-optimal set via MATLAB and then deploy a TOPSIS-based multi-criteria decision analysis to select the final design. An EMS is also developed to coordinate these components for reliable, cost-effective and sustainable operation.

Various metaheuristic algorithms have been employed for HRE sizing. However, they may suffer from premature convergence and limited solution diversity when applied to complex, high-dimensional design spaces. Although PSO, GA, and GWO have been widely utilized, as discussed in the literature review, no prior study has presented a direct comparative evaluation of these three algorithms within this specific context. To ensure a fair and unbiased assessment, a comparative analysis under identical settings is conducted. Many existing studies report optimization outcomes using different datasets, system configurations, parameter settings, or EMS strategies, which restricts direct comparability.

Accordingly, this study benchmarks PSO, GA, and GWO under the same objective functions, constraints, and operational conditions, while integrating rule-based energy management system (RB-EMS) to coordinate power dispatch and manage the charging and discharging cycles of the BT and HSS. The optimization framework minimizes three objectives: LCOE, PEC, and the introduced Grid Reliance Fraction (GRF), which quantifies grid dependency while incorporating electricity price and carbon intensity considerations. Furthermore, PSO, GA, and GWO are selected due to their widespread application and proven effectiveness in solving nonlinear, multi-objective HRE sizing problems. These algorithms represent distinct search paradigms, swarm intelligence, evolutionary genetics and social hierarchy-based hunting behavior. The main contributions of this study are delineated as follows:

- Development a grid-connected HRE system with PV, WT and hybrid hydrogen–battery storage system managed by a rule-based RB-EMS.
- Formulating a multi-objective function integrating LCOE, PEC and GRF for balanced economic, technical and environmental performance.
- To benchmark PSO, GA and GWO under identical conditions with the RB-EMS.
- Determining optimal sizing variables that maximize cost-effectiveness, resilience and sustainability.

2. CONFIGURATION AND SYSTEM MODELING

Figure 1 depicts the proposed HRE, which couples the utility grid with PV, WT and a hybrid hydrogen–battery storage system. All generators and storage units tie into a central DC bus; PV and WT through MPPT converter and rectifier, respectively. Similarly, the BT system via a charge controller while the Electrolyzer draws from the same bus for hydrogen production. Additionally, an inverter links the DC and AC buses, where the grid and local loads are connected. Detailed mathematical models of each component are provided in the next subsections.

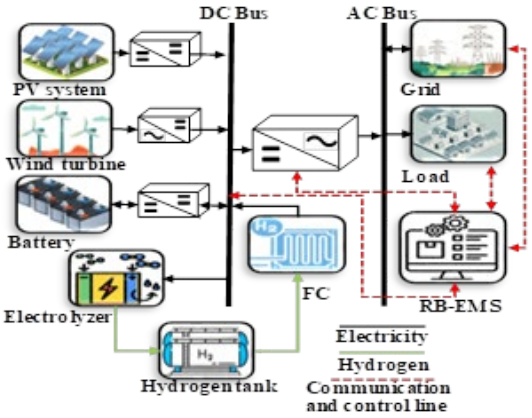

Figure 1. Schematic diagram of the proposed system

2.1 PV system

The power output of a PV system depends on the module's efficiency and local conditions such as solar irradiance and temperature. Based on these, the DC output power of the PV panel $P_{pv}(t)$ at time (t) can be modeled as follows [12]:

$$P_{pv}(t) = P_r \times G(t)/1000 \times \left[1 + T_c \times \left(T_A(t) + (T_n - 20/800) \times G(t)\right) - T_s\right] \quad (1)$$

where P_r, T_c, T_A, G, T_n and T_s demonstrate PV rated power, PV temperature coefficient ($-3.7 \times 10^{-3}\ 1/°C$), ambient temperature, irradiance, nominal operating temperature and PV temperature under standard test conditions, respectively. The proposed system in this study utilizes Peimar SG310MBF PV panel technology [6].

2.2 Wind system

The proposed design includes a wind turbine, optimally placed to support the PV arrays during low-sunlight periods. The turbine's electrical power output P_{WT}, obtained by converting wind kinetic energy, is expressed as [13]:

$$P_{WT(t)} = \begin{cases} Pw_r & v_R < v(t) < v_{cut_{out}} \\ Pwt_r \frac{v(t)-v_{cut_{in}}}{v_R - v_{cut_{in}}}, & v_{cut_{in}} < v(t) < v_R \\ 0 & otherwise \end{cases} \quad (2)$$

where Pw_r, v_R, v_r, $v_{cut_{in}}$, $v_{cut_{out}}$ represent wind turbine rated power, rated wind speed, wind speed, cut in wind speed and cut off wind speed, respectively. The Eocycle EO20 wind turbine is implemented in the proposed system of this work [14].

2.3 Battery storage system model

The BT system smooths power fluctuations from the PV panels and WTs under varying load. The grid-connected hybrid system in this study employs lithium-ion BT system for their high efficiency and lower cost. A surplus or deficit of energy, signifying charging or discharging, is defined by following [9]:

$$P_{Bat}(t) = P_{RE}(t) - (P_{laod}\ (t)/\eta_{in}) \quad (3)$$

where P_{Bat}, P_{RE}, P_{laod} and η_{in} demonstrate BT power, RE power (PV and WT), required load power and inverter efficiency, respectively. If $P_{Bat} > 0$, it indicates that the RE systems generate more power than is needed, while $P_{Bat} < 0$ indicates a power generation shortage. The BT system charges only when excess generation is available and its state of charge (SoC) is below the maximum (SoC_{max}). In contrast, the BT system discharges only when generation is insufficient and its SoC is above the minimum (SoC_{min}). Equations (4) and (5) represent the SoC of the BT system in charging and discharging, respectively [15]:

$$SoC(t) = SoC(t-1)(1-\alpha) + (P_{RE}(t) - (P_{load}(t))/\eta_{in}) \times \eta_{Bat} \quad (4)$$

$$SoC(t) = SoC(t-1)(1-\alpha) + ((P_{load}(t))/\eta_{in} - P_{RE}\ (t)) \times \eta_{Bat} \quad (5)$$

where, η_{Bat} is the BT efficiency and α represents the hourly self-discharge rate of the BT.

2.4 Hydrogen system model

In the hydrogen system model, the EL applies an electric current across electrodes separated by an electrolyte to split water into oxygen and hydrogen. Subsequently, the hydrogen flows into the hydrogen tank (HT) and onward to the FC to generate electricity. The power supplied by the EL to HT system is expressed as [9]:

$$P_{El}(t) = P_{RE\text{-}El}(t) \times \eta_{El} \quad (6)$$

where P_{El} is output power of EL, η_{El} is the EL efficiency and $P_{RE\text{-}El}$ represent the EL input power from RE generation. Hydrogen is compressed and stored in a high-pressure tank for later use in the FC. The Electrolyzer's hydrogen mass flow rate (MR_{H_2}), is calculated as:

$$MR_{H_2}(t) = \frac{P_{El}(t)}{Hv_{H_2}} \quad (7)$$

where Hv_{H_2} refer heating value of hydrogen, which is 39.72 kWh/kg [16]. Excess RES power first charges the BT storage system. Otherwise, instead of being sent to the grid, it is used for hydrogen production and stored in HT. The power stored in the hydrogen tank (P_{HT}) is given by:

$$P_{HT}(t) = P_{HT}(t-1) + P_{RE\text{-}El}(t) - P_{HT-Fc}(t) \times \eta_{HT} \quad (8)$$

where P_{HT-fc} denotes the supplied power to the FC from HT and η_{HT} represents the efficiency of HT.

The FC uses stored hydrogen to generate electricity for loads when renewables are low or demand peaks. The FC output power (P_{Fc}) is calculated by [15]:

$$P_{Fc}(t) = P_{HT-Fc}(t) \times \eta_{Fc} \times \eta_{con} \quad (9)$$

where the efficiencies of the FC and its converter are represented by η_{Fc} and η_{con}, respectively.

2.5 Modeling of utility grid and converter

Whenever renewable generation and storage cannot meet demand, the system imports power from the utility grid. Conversely, whenever generation and storage exceed demand, the surplus is exported to the utility grid. Imports are priced at \$0.17/kWh and exports at \$0.05/kWh, in line with Libya's post-subsidy tariff schedule [17]. Equally important, power converters bridge AC and DC components by converting current type. In this system, AC and DC sources share a common DC/AC bus via a Dynapower SPS-100 inverter, which offers 95 % efficiency, a 15-year lifespan, and annual maintenance equal to 1 % of its capital cost.

3. SYSTEM PROPOSED CONTROL STRATEGY

A rule-based EMS governs energy flow by applying conditional decisions that favor renewable sources over the utility grid. Its dispatch hierarchy is renewable generation, PV and WT, BT system, HSS and grid supply as a last resort. This dynamic coordination enhances system efficiency and reliability by ensuring the grid is used only when on-site resources cannot meet demand. In order to accomplish this, the following steps will be taken to operate the microgrid [9]:

- Condition 1 If RES generation equals to demand ($P_{pv}(t) + P_{wt}(t) = P_{load}(t)$), RE sources fully supply the load.
- Condition 2 When $P_{pv}(t) + P_{wt}(t) > P_{load}(t)$ and the

battery's SoC is below its maximum ($\mathrm{SoC}(t) < \mathrm{SoC}_{max}$), excess energy is stored in the battery.

- Condition 3 If $\mathrm{SoC}(t) \geq \mathrm{SoC}_{max}$, surplus renewable power charges the Electrolyzer for HSS; any remaining excess is exported to the grid.
- Condition 4 When $P_{pv}(t) + P_{wt}(t) < P_{load}(t)$, the BT discharges to meet the shortfall.
- Condition 5 If RE plus BT discharge still fall short, the FC and BT system jointly supply the remaining demand.
- Condition 6 If RES generation, BT and FC together cannot meet the load, the utility grid provides the deficit.

The operational strategy of the HRE system based on RB-EMS is presented in simplified flowchart in Figure 2.

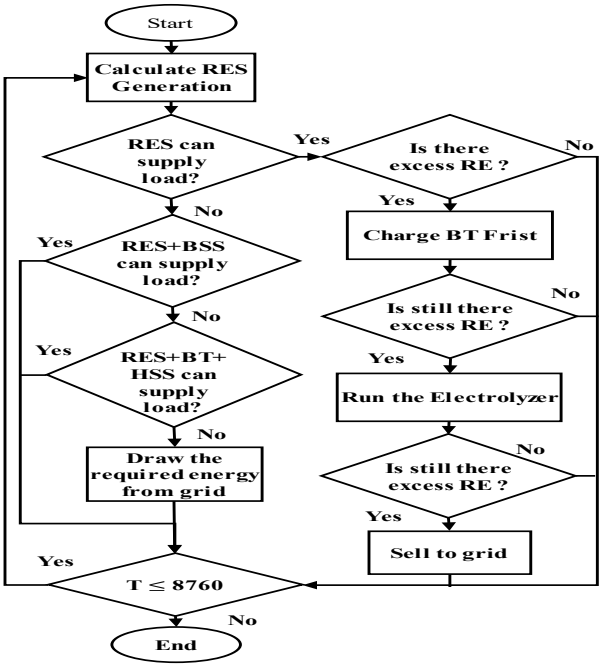

Figure 2. The operational RBEMS strategy of the system.

4. OBJECTIVES FUNCTION

The optimization framework defines three key objectives for sizing the HRE microgrid: LCOE, GRF and PEC. These are combined into one function (f) to balance cost, grid reliance and emissions as [18]:

$$min\ F = \sum_{j=1}^{n} f_j \times w_j \tag{10}$$

where j represents each of the n objective functions f_j, while w_j denotes a nonnegative weight for each xth objective function. In this study, the objective weights in Eq. (10) are predefined and kept constant throughout the optimization process. The weights are set to $w_1 = 0.7$ for LCOE, $w_2 = 0.2$ for GRF, and $w_3 = 0.1$ for PEC, reflecting the higher priority given to economic performance in grid-connected applications, while still accounting for grid dependency and environmental impact. This weighting scheme is consistent with the practical objectives of the Libyan case study, where cost reduction and energy security are dominant concerns [19,17].

The LCOE is a key metric for assessing the economic viability of the HRE system. It accounts for all lifecycle costs, including initial capital (ICC), replacement (RC), maintenance and operation (M&O) costs. LCOE is calculated as the ratio of the TAC to the sum of annual energy consumed by the load (E_{load}) and sum energy sold to the grid (Eg_{out}) as follows [17,19]:

$$LCOE = \frac{TAC}{\sum_{t=1}^{8760}(E_{load} + Eg_{out})} \tag{11}$$

$$TAC = NPC \times CRF + Cg_{net} \tag{12}$$

$$Cg_{net} = Eg_{in} \times C_b - Eg_{out} \times C_s \tag{13}$$

Here, Cg_{net} represents the net grid energy cost, calculated by subtracting revenue from energy sold to the grid from the total cost of bought electricity. Eg_{in} represents the sum energy purchased from the utility grid. C_b, C_s and CRF denote the purchase price, selling price and capital recovery factor, respectively. The NPC accounts for the present value of all costs associated with each distributed generation source, including ICC, RC and M&O costs. NPC is represented as [6]:

$$NPC = \sum_i \left[N_{DG}^i \times ICC_{DG}^i\right] + \sum_i \left[N_{DG}^i \times RC_{DG}^i\right] + \frac{1}{CRF} \times \sum_i \left[N_{DG}^i \times M\&O_{DG}^i\right] \tag{14}$$

where, N_{DG}^i denotes the optimal capacity of each distributed generation (DG) source, with i indicating the different DG types in the HRE system, each having specific ICC, RC and M&O cost.

Grid Reliance Fraction (GRF), the second minimized objective, measures the share of total energy demand met by the utility grid. It is calculated as the ratio of imported grid energy Eg_{in} to total load E_{load}. A lower GRF indicates higher self-sufficiency and reduced emissions, supporting energy security and sustainability [21].

$$GRF = \frac{\sum_{t=1}^{8760} Eg_{in}}{\sum_{t=1}^{8760} E_{load}} \times 100 \tag{15}$$

Pollutant Emission Coefficient (PEC) is third minimized objective, represents the total CO_2 emissions, indicating the system's environmental impact. This study considers CO_2 emissions, the primary greenhouse gas from the energy sector. Total CO_2 emissions and PEC are calculated as follows [17]:

$$CO_2 = \sum_k \gamma_{EF}^k \times E_{DG}^k + \gamma_{EF}^{Grid} \times Eg_{in} - \gamma_{EF}^{Grid} Eg_{out} \tag{16}$$

The emission factor and total energy of the DG set are denoted by γ_{EF}^i and E_{DG}^i, respectively.

5. SYSTEM SIZING USING METAHEURISTIC ALGORITHMS

Three metaheuristic algorithms are applied to the optimal size of HRE system. The three algorithms PSO, GA and GWO differ in how they create new populations. In PSO [13], each particle updates its velocity and position by learning from its own best position and the swarm's global best. In GA [22], selection picks high-fitness individuals, crossover recombines their genes which are component sizes in this study, and mutation introduces random variations. In GWO [23], candidate solutions which is wolves adjust their positions by mimicking the social hierarchy and hunting behavior of grey wolves, with alpha, beta and delta wolves guiding the movement of the pack. Table 1 delineates the specific parameter combinations of the employed algorithms. All three algorithms follow the same evaluation and replacement loop and are terminated after a fixed maximum of 100 iterations, as shown in Figure 3. The flowchart outlines a unified metaheuristic optimization framework used to size the HRE system.

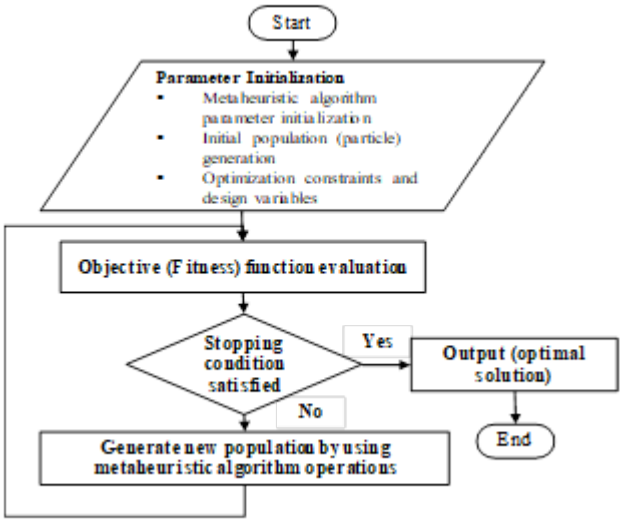

Figure 3. Flowchart of the implemented metaheuristic optimization algorithms.

Table 1. The particular parameter settings of employed algorithms.

PSO algorithm	GA algorithm	GWO algorithm
Size of population $N = 20$	Size of population $N = 20$	Size of population $N = 20$
Iteration i = 100	Iteration i = 100	Iteration $i = 100$
Inertia weight $\mathcal{W}$ = 0.7	Mutation distribution index: 20	$r_1 \in [0,1]$ $r_2 \in [0,1]$
Cognitive coefficient $\mathcal{C}1$ = 1.5	Crossover distribution index: 20	$a = [2\ to\ 0]$
Social coefficient $\mathcal{C}2$ = 1.5	Mutation Rate = 0.2	Wolf hunting technique, directed by the Alpha
Velocity clamping parameter $\mathcal{V}_{max}$ = 0.2	Crossover Rate = 0.8	

6. RESULTS AND DISCUSSION

A size-optimized grid-connected HRE, comprising PV panels, WT, HSS, and a BT storage system, was developed to meet the energy needs of the Dahra Field Camp, operated by Waha Oil Company near Sirte, Libya (29.48233° N, 17.92266° E). Annual environmental data: temperature, solar irradiation and wind speed from the Global Sun Atlas were employed as shown in Figure 4a-c. The camp's load profile, which includes workshops, a kitchen, gas and water plants and residential buildings, was used to size and optimize the system as shown in Figure 5.

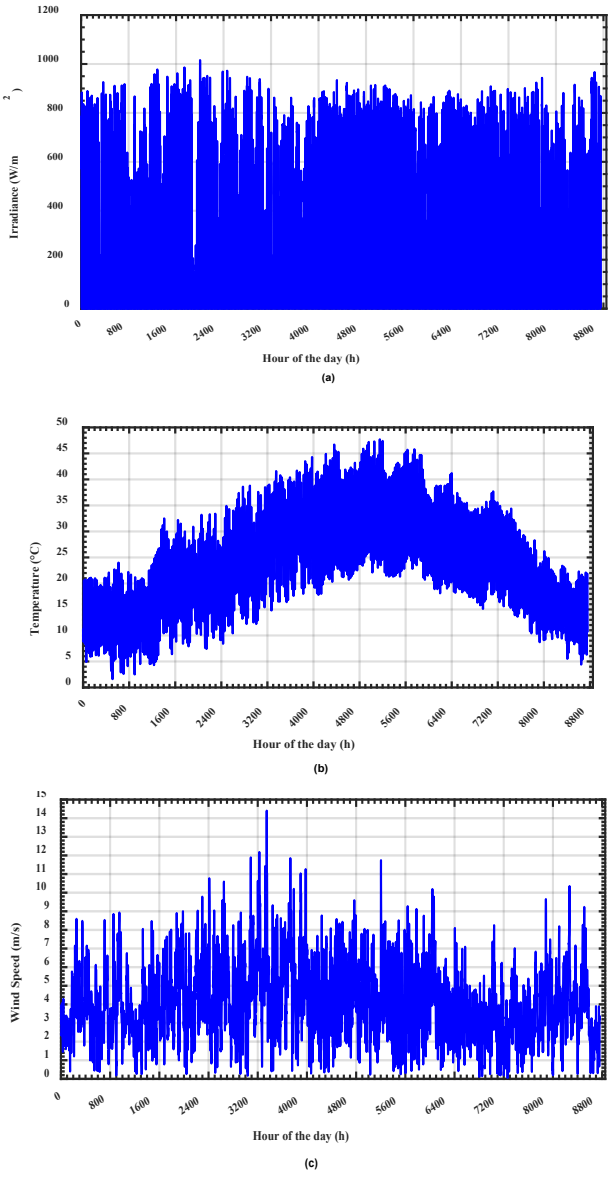

Figure 4. Annual site data: (a) solar irradiation, (b) ambient temperature, (c) wind speed

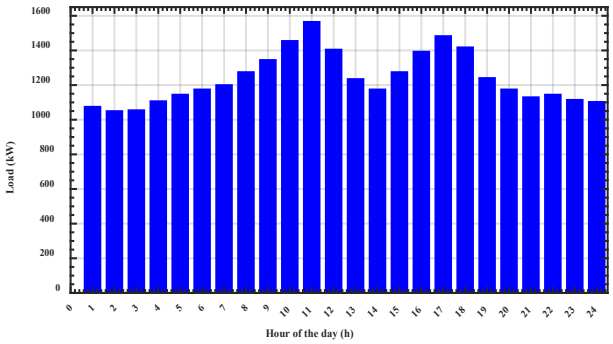

Figure 5. Input features of the daily load profile

Table 2 presents the results of three size optimization algorithms; PSO, GA and GWO, used to optimize techno-economic performance and system capacity in a typical HRE system, consisting of PV, WT, BSS, EL, HT, and FC. Key performance indicators include the LCOE, GRF and PEC. A lower LCOE indicates better economic viability. The PSO algorithm achieved the lowest LCOE at \$0.1448/kWh, outperforming GA (\$0.1684/kWh), GWO (\$0.1464/kWh), as shown in Table 2.

The GRF quantifies dependence on the utility grid, lower values denote higher system autonomy. As shown in Table 2, PSO, GA and GWO achieve GRFs of 15.73 %, 16.59 % and 16.51 %, respectively, with PSO exhibiting the least grid dependent. The PSO-based optimum design comprises a 6000 kW PV array, 40 kW WT, 1070 kW FC, 8800 kWh BT storage, 2160 kW EL and 638 kg HT resulting in a configuration in which solar generation predominates over wind.

Table 2. Optimal results of PSO, GA and GWO Algorithms

Parameter	PSO	GA	GWO
LCOE (\$/kWh)	0.1448	0.1684	0.1464
GRF (%)	15.73	16.59	16.51
PEC (kg/kW)	0.1264	0.0494	0.1354
NPC (\$)	1.3442×10^7	1.564×10^7	1.3594×10^7
PV (kW)	6000	5877	5800
WT (kW)	40	1080	240
BT (kW)	8800	9300	8500
EL (kW)	2160	1985	1962
HT (kg)	638	715	685
FC (kW)	1070	911	1211

The assessment of optimization algorithms reveals variations in convergence properties. Figure 6 compares the best-fitness evolution over 100 iterations for PSO, GA and GWO, showing that although all three steadily improve, PSO converges more rapidly and smoothly by effectively balancing exploration and exploitation to avoid local minimum. In contrast, GA and GWO exhibit slower, irregular fitness declines, reflecting weaker exploitation of promising regions and a higher risk of settling in suboptimal solutions.

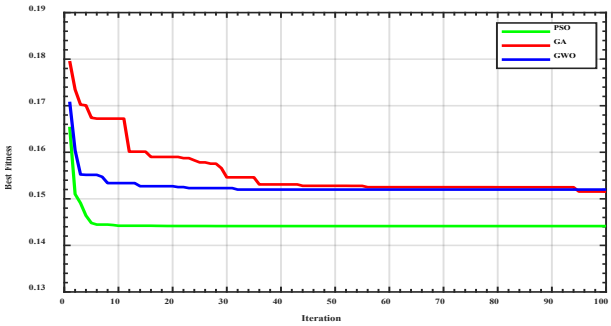

Figure 6. The convergence behaviour of different optimization algorithms.

To evaluate algorithms robustness, each metaheuristic was executed over multiple runs, and the mean and standard deviation (STD) of the objective functions are summarized in Table 3.

Table 3. Statistical performance of metaheuristic algorithms

Parameters		PSO	GA	GWO
Mean	LCOE (\$/kWh)	0.1476	0.1752	0.1478
	GRF (%)	15.67	18.63	17.82
	PEC (kg/kW)	0.1360	0.1026	0.1102
STD	LCOE (σ)	0.00288	0.0103	0.0026
	GRF (σ)	0.448	2.16	1.34
	PEC (σ)	0.01784	0.0407	0.0421

Based on the PSO-driven optimal design, different energy sources follow distinct generation profiles, and their combined output is crucial for meeting total demand. Figure 7 shows first 4-day power flows in the HRE system under the RB-EMS, where load is served by PV-WT generation, BT charging/discharging, FC, EL and grid exchange. Residential demand remains high at night, while daytime usage rises from workshops and kitchens. PV-WT output fluctuates, peaking between 10-15 hours. BT power switches between discharge (negative) and charge (positive) to balance supply, and grid exchange alternates between import and export. During low renewable output, such as nighttime or cloudy periods, the grid supplies the deficit. Overall, the RB-EMS dynamically coordinates all components to maximize RES and ensure reliable supply.

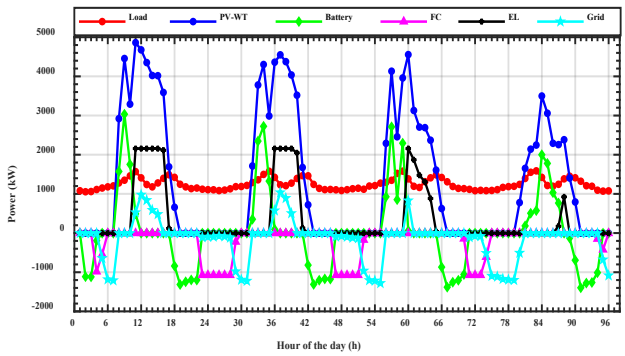

Figure 7. Energy balance and power generation mix based on PSO-driven optimal design

During the four-day span depicted in Figure 8, the system consistently extracts power from the grid during periods of low demand and exports excess energy during peak renewable output, as indicated by the curve crossing above and below zero. Similarly, the hydrogen curve illustrates how the Electrolyzer charges HT when excess RE power is available and how the FC discharges stored energy during peak demand. Consequently, the SOC follows a sawtooth pattern: rising sharply during charging phases to 90 %, then gradually declining as energy is drawn from the BT storage system. This coordinated operation smooths grid interaction and maintained SOC within safe bounds, demonstrating effective management of renewable generation and storage resources.

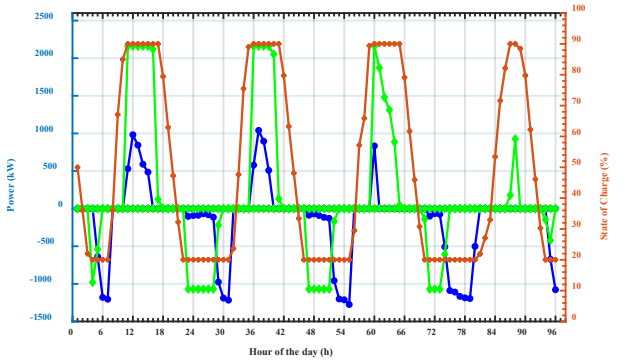

Figure 8. Dynamics of grid exchange, hydrogen tank energy flow and SOC for 4-day.

7. CONCLUSION

This study proposes an optimization framework for sizing a grid-connected HRE system using three metaheuristic algorithms. The framework determines optimal capacities for PV, WT, BT storage systems, FC, EL and HT while simultaneously addressing cost efficiency, energy reliability and environmental sustainability. Its primary objective is to secure a consistent annual power supply for the Dahra Field Camp in southeastern Libya over a 25-year lifespan, minimizing the LCOE, GRF and PEC. The proposed design effectively balances technical, economic and ecological goals. Among the three algorithms tested, PSO most successfully avoided premature convergence and identified superior solutions. PSO achieved the lowest LCOE of $0.1448/kWh, compared with $0.1464/kWh for the GWO and $0.1684/kWh for GA. It also reduced the GRF to 15.73%, meaning the system draws just 15.73% of its annual energy from the utility grid, dramatically cutting emissions and enabling near off-grid operation. These results demonstrate the value of metaheuristic algorithms as robust tools for designing resilient, cost-effective grid-connected HRE systems. Future work could extend this framework to fully off-grid configurations and investigate the integration of electric vehicles for additional flexibility and load management work or suggest applications and extensions.

ACKNOWLEDGMENT

The authors gratefully acknowledge financial support from the Ministry of Higher Education, Universiti Teknologi Malaysia, under the Fundamental Research Grant Scheme (FRGS/1/2021/TK0/UTM/02/19). We also thank Universiti Teknologi Malaysia for providing comprehensive facilities and our colleagues for directly or indirectly their contributions. The first author would like to thank the Libyan Ministry of Higher Education for providing a scholarship to support this work.

REFERENCES

[1] K. Ghanbari, A. Maleki, and D. Rezaei Ochbelagh, “Investigating the effect of various types of components in optimal designing of a solar/wind/storage hybrid system,” *J. Energy Storage*, vol. 110, no. June 2024, Art. no. 135, 2025, doi: 10.1016/j.est.2024.115273.

[2] M. Almaktar and M. Shaaban, “Prospects of renewable energy as a non-rivalry energy alternative in Libya,” *Renew. Sustain. Energy Rev.*, vol. 143, no. February, p. 110852, 2021, doi: 10.1016/j.rser.2021.110852.

[3] A. Alsharif *et al.*, “Impact of Electric Vehicle on Residential Power Distribution Considering Energy Management Strategy and Stochastic Monte Carlo Algorithm,” *Energies*, vol. 16, no. 3, Art. no. 050A, 2023, doi: 10.3390/en16031358.

[4] M. F. Hamza and B. Modu, “A bibliometric analysis on renewable energy microgrids integrating hydrogen storage: Strategies for optimal sizing and energy management,” *Sci. African*, vol. 27, no. January, p. e02609, 2025, doi: 10.1016/j.sciaf.2025.e02609.

[5] Y. He, S. Guo, P. Dong, Y. Zhang, J. Huang, and J. Zhou, “A state-of-the-art review and bibliometric analysis on the sizing optimization of off-grid hybrid renewable energy systems,” *Renew. Sustain. Energy Rev.*, vol. 183, no. October 2022, Art. no. 165, 2023, doi: 10.1016/j.rser.2023.113476.

[6] V. Dargahi, H. HassanzadehFard, F. Tooryan, and F. Tourian, “Reliable cost-efficient integration of pumped hydro storage in islanded hybrid microgrid for optimum decarbonization,” *Energy*, vol. 312, no. August 2023, Art. no. 015, 2024, doi: 10.1016/j.energy.2024.133615.

[7] C. Yan, Y. Zou, Z. Wu, and A. Maleki, “Effect of various design configurations and operating

conditions for optimization of a wind/solar/hydrogen/fuel cell hybrid microgrid system by a bio-inspired algorithm," *Int. J. Hydrogen Energy*, vol. 60, no. February, Art. no. 018, 2024, doi: 10.1016/j.ijhydene.2024.02.004.

[8] M. Agoundedemba, C. K. Kim, H. G. Kim, R. Nyenge, and N. Musila, "Modelling and optimization of microgrid with combined genetic algorithm and model predictive control of PV/Wind/FC/battery energy systems," *Energy Reports*, vol. 13, no. August 2024, Art. no. 003, 2025, doi: 10.1016/j.egyr.2024.12.008.

[9] B. Modu, M. P. Abdullah, A. AlKassem, M. F. Hamza, and A. L. Bukar, "The role of hybrid hydrogen-battery storage in a grid-connected renewable energy microgrid considering time-of-use electricity tariffs," *J. Energy Storage*, vol. 105, no. November 2024, Art. no. 001, 2025, doi: 10.1016/j.est.2024.114729.

[10] A. I. Abeg, M. R. Islam, M. A. Hossain, M. F. Ishraque, M. R. Islam, and M. J. Hossain, "Capacity and operation optimization of hybrid microgrid for economic zone using a novel meta-heuristic algorithm," *J. Energy Storage*, vol. 94, no. June, p. 112314, 2024, doi: 10.1016/j.est.2024.112314.

[11] H. Yazdani, M. Baneshi, and M. Yaghoubi, "Techno-economic and environmental design of hybrid energy systems using multi-objective optimization and multi-criteria decision making methods," *Energy Convers. Manag.*, vol. 282, no. March, Art. no. 019, 2023, doi: 10.1016/j.enconman.2023.116873.

[12] M. Ganbasha and R. Ayop, *Sizing of Standalone Photovoltaic-Thermoelectric Cogeneration System Using Particle Swarm Optimization*, vol. 921 LNEE. Springer Nature Singapore, 2022. doi: 10.1007/978-981-19-3923-5_40.

[13] L. El Boujdaini, A. Mezrhab, M. A. Moussaoui, F. Jurado, and D. Vera, "Sizing of a stand-alone PV–wind–battery–diesel hybrid energy system and optimal combination using a particle swarm optimization algorithm," *Electr. Eng.*, vol. 104, no. 5, pp. 3339–3359, 2022, doi: 10.1007/s00202-022-01529-0.

[14] M. Katsivelakis, D. Bargiotas, A. Daskalopulu, I. P. Panapakidis, and L. Tsoukalas, "Techno-economic analysis of a stand-alone hybrid system: Application in donoussa island, greece," *Energies*, vol. 14, no. 7, Art. no. 029, 2021, doi: 10.3390/en14071868.

[15] B. Modu, M. P. Bin Abdullah, A. Alkassem, H. Z. A. Garni, and M. Alkabi, "Optimal Design of a Grid-Independent Solar-Fuel Cell-Biomass Energy System Using an Enhanced Salp Swarm Algorithm Considering Rule-Based Energy Management Strategy," *IEEE Access*, vol. 12, no. January, Art. no. 044, 2024, doi: 10.1109/ACCESS.2024.3362241.

[16] B. Modu, M. P. Abdullah, A. L. Bukar, M. F. Hamza, and M. S. Adewolu, "Energy management and capacity planning of photovoltaic-wind-biomass energy system considering hydrogen-battery storage," *J. Energy Storage*, vol. 73, no. PD, Art. no. 046, 2023, doi: 10.1016/j.est.2023.109294.

[17] A. Elbaz and M. T. Guneser, "Multi-Objective Optimization Method for Proper Configuration of Grid-Connected PV-Wind Hybrid System in Terms of Ecological Effects, Outlay, and Reliability," *J. Electr. Eng. Technol.*, vol. 16, no. 2, Art. no. 077, 2021, doi: 10.1007/s42835-020-00635-y.

[18] A. Al-Quraan and B. Al-Mhairat, "Sizing and energy management of grid-connected hybrid renewable energy systems based on techno-economic predictive technique," *Renew. Energy*, vol. 228, no. May, Art. no. 005, 2024, doi: 10.1016/j.renene.2024.120639.

[19] Y. F. Nassar, H. J. El-Khozondar, and M. A. Fakher, "The role of hybrid renewable energy systems in covering power shortages in public electricity grid: An economic, environmental and technical optimization analysis," *J. Energy Storage*, vol. 108, no. December 2024, p. 115224, 2025, doi: 10.1016/j.est.2024.115224.

[20] A. F. N. ; M. O. Gu, "Multi-objective optimization and sustainable design : a performance comparison of metaheuristic algorithms used for on-grid and off-grid hybrid energy systems," vol. 2, Art. no. 109, 2024, doi: 10.1007/s00521-024-09585-2.

[21] M. Ganbasha, R. Ayop, M. J. A. Aziz, Mohd Rodhi Bin Sahid, Mohammad Al Takrouri, and Firdaus Ishak, "Optimal design and techno-economic-environmental evaluation of hybrid renewable energy-based microgrid system using moss growth optimization", doi: 10.2139/ssrn.5225962.

[22] R. Dufo-López, J. M. Lujano-Rojas, and J. L. Bernal-Agustín, "Optimisation of size and control strategy in utility-scale green hydrogen production systems," *Int. J. Hydrogen Energy*, vol. 50, Art. no. 028, 2024, doi: 10.1016/j.ijhydene.2023.08.273.

[23] D. K. Geleta, M. S. Manshahia, P. Vasant, and A. Banik, "Grey wolf optimizer for optimal sizing of hybrid wind and solar renewable energy system," *Comput. Intell.*, vol. 38, no. 3, pp. 1133–1162, 2022, doi: 10.1111/coin.12349.